al Research Laboratory

ton, DC 20375-5000

NRL Memorandum Report 6750

AD-A779 808

Simulation Studies of a Klystronlike Amplifier Operating in the 10-100 GW Regime

J. KRALL, M. FRIEDMAN, Y. Y. LAU AND V. SERLIN

Beam Physics Branch
Plasma Physics Division

November 20, 1990

DTIC
ELECTE
DEC 04 1990
S
B
D

REPORT DOCUMENTATION PAGE

1. AGENCY USE ONLY (Leave blank)	2. REPORT DATE 1990 November 20	3. REPORT TYPE AND DATES COVERED Interim

4. TITLE AND SUBTITLE

Simulation Studies of a Klystronlike Amplifier Operating in the 10-100 GW Regime

5. FUNDING NUMBERS

SDIO/IST
JO # 47-3593-00

6. AUTHOR(S)

J. Krall, M. Friedman, Y. Y. Lau and V. Serlin

7. PERFORMING ORGANIZATION NAME(S) AND ADDRESS(ES)

Naval Research Laboratory
Code 4790
Washington, DC 20375-5000

8. PERFORMING ORGANIZATION REPORT NUMBER

NRL Memorandum
Report 6750

9. SPONSORING/MONITORING AGENCY NAME(S) AND ADDRESS(ES)

SDIO/LST
Harry Diamond Laboratory
Adelphi, MD 20783

10. SPONSORING/MONITORING AGENCY REPORT NUMBER

11. SUPPLEMENTARY NOTES

12a. DISTRIBUTION/AVAILABILITY STATEMENT

Approved for public release; distribution unlimited.

12b. DISTRIBUTION CODE

13. ABSTRACT (Maximum 200 words)

A coaxial drift tube allows propagation of an ultra high power relativistic electron beam (500 keV, $\geq$ 100 kA, 100 ns). In this paper we study the modulation on a large diameter (12.6 cm) intense relativistic electron beam (500 keV, 16 ka) by an external microwave source via particle simulation. The annular beam, enclosed within a coaxial drift tube, is found to be fully modulated by a low-power external rf source at a frequency of 1.3 GHz. We show that for such an intense beam, a highly nonlinear interaction takes place at the modulating gap, producing highly coherent bunches of electrons. This finding is similar to earlier research in which such modulation was studied for an intense beam propagating in a *hollow* drift tube. We further show that, unlike the hollow drift tube case, the coaxial configuration is easily scaled to high power. here, a very large diameter (26 cm) intense beam (460 keV, 100 kA) is fully modulated at 1.3 GHz to obtain 31 GW of rf beam power.

14. SUBJECT TERMS

High power microwaves · Relativistic klystron amplifiers
Intense beam modulation

15. NUMBER OF PAGES

30

16. PRICE CODE

17. SECURITY CLASSIFICATION OF REPORT	18. SECURITY CLASSIFICATION OF THIS PAGE	19. SECURITY CLASSIFICATION OF ABSTRACT	20. LIMITATION OF ABSTRACT
UNCLASSIFIED	UNCLASSIFIED	UNCLASSIFIED	SAR

CONTENTS

SIMULATION STUDIES OF A KLYSTRONLIKE AMPLIFIER OPERATING IN THE 10-100 GW REGIME

I. Introduction

Recent experiments at the U.S. Naval Research Laboratory have shown that a hollow annular intense relativistic electron beam could be fully modulated by a moderate external rf source at a frequency f = 1.3 GHz and that the interaction of this beam with a structure generated a 3 GW rf pulse that was radiated into the atmosphere.[1] Several unusual properties were discovered in these and in previous experiments[1-3] namely, the high degree of phase and amplitude stability in the output signal, the ease with which the current modulation can be achieved and controlled, and the avoidance of electrical breakdown at the gaps, even at high modulation levels.

The experimental configuration consisted of an annular beam (r_b = 6.6 cm, I = 16 kA, V_o = 500 kV) propagating within a hollow drift tube (r_w = 7.0 cm). A gap in the drift tube fed into a coaxial radial cavity, which was energized by an external rf source with power ~ 0.5 MW. This cavity partially modulated the beam. A second radial cavity, 30 cm downstream, was energized by the partially modulated beam in such a way as to obtain a fully modulated beam immediately following the second gap. Both cavities were tuned to a frequency f = 1.3 GHz.

The interaction between the beam and each of the external cavities has been studied in some detail in both the linear and nonlinear regimes.[1,3,4] The deviations in these interactions from the classical klystron arise from the intense space charge of the beam and the fact that the kinetic, rf, and potential energy of the beam are all of the same order of magnitude, rendering the classical picture of beam bunching invalid.

Recent efforts have been directed toward increasing the rf power of the modulated intense relativistic electron beam (MIREB).[5] Naturally,

increasing the dimensions of the drift tube and the beam would allow a higher beam current. However, the use of a hollow drift tube dictates the permissible size as the drift tube radius must be small enough that the TM_{01} waveguide mode is cut off at the frequency of modulation.

To overcome these limitations, a <u>coaxial</u> geometry has been proposed.[6] This is shown schematically in Fig. 1. This configuration has two major advantages: a) the limitation on the outer wall radius is relaxed as long as the inner and outer walls are sufficiently close and b) the limiting current in a coaxial geometry is approximately twice as large as in a hollow drift tube. These features of the coaxial geometry allow propagation of beam currents in the 100 kA range. The advantage of electrostatic insulation at the gap is retained in this new configuration. The major issue, which is favorably resolved in this paper, is that the beam can be modulated with good efficiency and phase and amplitude stability, in spite of the fact that TEM modes are admissible solutions in a coaxial geometry. That is, despite the possible presence of TEM modes, the cavities must remain isolated electromagnetically as far as the beam-cavity interactions are concerned.

In this configuration (see Fig. 1) an annular IREB is generated and guided throughout by a 10 kG axial magnetic field. The IREB enters the drift region between the outer drift tube wall and the large radius center conductor, both of which are grounded. One or more pairs of radial cavities are exposed to the drift region via gaps in the inner and outer walls. A moderate power external source "pumps" rf power into one or more of these cavities. The IREB, which is partially modulated by these driven cavities, resonantly excites subsequent cavities so as to produce a fully

modulated beam. The rf power of the modulated IREB (MIREB) may then be extracted.

Note that this coaxial geometry is quite similar to the sheet-beam klystron of Eppley et al.[7] In the sheet beam klystron the geometry was also motivated by the need to increase the total beam current while maintaining a low current density. This allows the sheet beam klystron to avoid space charge effects and thus behave like a classical klystron. This is contrary to our case, in which the space charge effects of the intense beam are beneficial (for bunching and electrostatic insulation) as was suggested repeatedly by our previous experimental, theoretical and numerical results.

In this study we consider a coaxial design with only two cavities, the first of which is externally driven. We will first choose parameters for which the TM_{01} mode is cut off even if the center conductor is removed, so as to obtain direct comparisons between the hollow and coaxial geometries. We discuss the theoretical differences between the two geometries and present numerical results. Finally, we show that the new geometry is easily scalable to high power by significantly increasing the diameter and current of the annular beam.

II. Beam Modulation in Coaxial Geometry

The physics of IREB modulation in a hollow drift tube geometry was discussed in an earlier article.[3] Here we will concentrate on the way the presence of the center conductor changes the bunching mechanism in the linear and nonlinear regimes. Again we consider a two cavity system in which only the first is externally driven. The bunching mechanism at each of the two gaps is strongly influenced by the electric and magnetic fields

3

of the intense beam. At high current levels, the potential energy of the beam may be a sizable fraction of its kinetic energy. We find

$$\gamma_{inj} = \gamma_0 + I_0/I_s\beta_0 \approx \gamma_0 + \alpha_0\gamma^3 \tag{1}$$

where

$$\alpha_0 = I_0/(I_s\gamma_0^3\beta_0) \, , \tag{2}$$

$$I_s = 2\pi\varepsilon_0\frac{m_0c^3}{e}\left[\frac{1}{\ln(r_w/r_b)} + \frac{1}{\ln(r_b/r_c)}\right] \, , \tag{3}$$

I_0 is the IREB current, $m_0c^2(\gamma_0-1)$ is the electron kinetic energy, $\gamma_0 = (1-\beta_0^2)^{-1/2}$, $\beta_0 = v_0/c$, v_0 is the electron drift velocity, $eV_0 = m_0c^2(\gamma_{inj}-1)$ is the electron total energy at injection, and r_w, r_b and r_c are the respective radii of the drift tube, the annular beam and the center conductor. At a current level I_c, where

$$I_c = I_s(\gamma_{inj}^{2/3} - 1)^{3/2} \tag{4}$$

the beam has zero kinetic energy and beam propagation is disrupted.

Note that except for the scale current, I_s, these relations describe the beam in the hollow as well as the coaxial configurations. In the hollow drift tube case, $I_s = 2\pi\varepsilon_0 m_0c^3/e\ln(r_w/r_b)$, where r_w is the drift tube radius. In the situation where $r_c \ll r_w$, r_b the two cases are nearly identical. For a large radius center conductor which we will consider here, $r_w - r_b \simeq r_b - r_c \ll r_b$ and we find that $I_s[coaxial] \simeq 2I_s[hollow]$. This means that relative to the hollow drift tube, the coaxial configuration carries less potential energy. Equivalently, the parameter α

4

in Eq. (1) is reduced by approximately a factor of two by the presence of the large-radius center conductor.

The effect of the first, externally-driven cavity in this device is to excite linear fast and slow space charge waves on the beam. Except for the parameter α, the dispersion relation for these waves is identical to the relation already derived for the hollow drift tube case[8,9,3] and will not be rederived here. We merely quote the result that with the boundary conditions at the first gap, $I_1 = 0$ and $V_1 = V_{10}\exp(j\omega t)$ one obtains the modulated current and voltage at $z = z_1$:

$$I_1 = j\frac{V_{10}}{Z}\sin(\alpha\mu\theta_1) \qquad \theta_1 = \frac{\omega\delta z_1}{\beta_0 c} \tag{5}$$

$$V_1 = V_{10}[\cos(\alpha\mu\theta_1) + j\zeta\sin(\alpha\mu\theta_1)] , \tag{6}$$

where ω is the radian frequency of the external rf voltage,

$$\alpha\mu = (\alpha^2 + \alpha/\gamma_0^2)^{1/2}/\beta_0 , \tag{7}$$

$$\delta = \beta_0^2/(\beta_0^2 - \alpha) , \tag{8}$$

$$\zeta = (1 - \delta)/\alpha\mu\delta \quad (\zeta<0), \tag{9}$$

and

$$Z = m_0 c^2 \gamma_0^3 \beta_0^2 \alpha\mu/eI_0 . \tag{10}$$

In a typical case, α is small compared to unity and γ_0 is moderate such that $\alpha\mu \sim \alpha^{1/2}$. We see that for the coaxial case, relative to the hollow

drift tube case, α' decreases slightly. This has the effect of increasing by this same factor ($\simeq 2^{1/2}$ in our "typical case") both the drift length required for peak linear modulation and the amplitude of the modulation. The relatively small modulation level from the first gap serves to excite a strongly nonlinear interaction at the second gap. Because previous experimental and numerical results show that the second gap interaction is not a strong function of V_{10}[3,10], small changes in the linear regime modulation are expected to have a minimal impact on the final modulation level.

The interaction at the second gap, wherein the partially modulated beam resonantly excites the second cavity to obtain a very high voltage, has been previously studied in some detail.[3,11] As in the linear regime, the nonlinear interaction in the coaxial geometry closely resembles that of the the hollow drift tube case. The most significant difference governs the voltage that must be sustained on the second gap before the gap voltage stops the forward propagation of the slow space charge wave, resulting in strong current modulation immediately beyond the gap exit. Strong current modulation without the need of a drift region is a unique property of an intense beam.

Through a self-consistent nonlinear formulation for space charge waves on an intense beam in the long-wavelength approximation, it has been shown that when the local current perturbation is large enough to stop the propagation of the slow space charge wave, the local drift speed of the electrons v_{Nm} is determined by solving

$$\beta_{Nm}^2 \gamma_{Nm}^3 = I_0/I_s\beta_0 . \tag{11}$$

where $\gamma_{Nm} = (1 - \beta_{Nm}^2)^{-1/2}$ and $\beta_{Nm} = v_{Nm}/c$. The threshold voltage at the gap required for this to occur has been estimated and is given by

$$V_{th} = \frac{m_0 c^2}{e} \{\gamma_{inj} - [1 + (\frac{I_0}{I_s})^{2/3}]^{3/2}\} . \qquad (12)$$

When the gap voltage, V_1, exceeds V_{th}, we obtain rf current at the gap exit:

$$(I_1)_{exit} \simeq I_0 (2/\pi)(1 - V_{th}^2/V_1^2)^{1/2} . \qquad (13)$$

Physically, for $V_1 > V_{th}$, the propagation of the slow space charge wave is interrupted once per cycle, during which time the beam slows to $\beta = \beta_{Nm}$. The gap thus acts as a "gate" for the beam current. This rather simple physical model is discussed in greater detail in Ref. 3.

The increase in I_s in the coaxial geometry (relative to the hollow geometry) will have the effect of lowering β_{Nm} and increasing V_{th} but, unlike the linear regime, it is not clear how this will effect the resulting modulation. These effects if any, will be seen in the simulation results below.

III. Numerical Results

We use CONDOR[12], a fully electromagnetic, fully relativistic particle simulation code, to simulate IREB generation in two dimensional (r,z) geometries. In simulating the hollow drift tube and coaxial geometries, we wish to learn, firstly, how the presence of the center conductor effects the nonlinear behavior as discussed above and, secondly, to what degree, if any, do the radial cavities couple to the TEM coaxial waveguide mode. This

second question is of the utmost importance, since coupling to the TEM mode would considerably weaken the modulating action by the individual cavities and may even allow rf energy from the cavities to propagate out of the system. These processes would be disastrous to the beam-gap interactions.

Here, we directly compare modulation in the coaxial and hollow drift tube geometries for identical parameters. The hollow drift tube geometry in is shown in Fig. 2; the coaxial geometry, with the added center conductor, is also shown. The outer wall radius is r_w = 6.8 cm, the beam radius is r_b = 6.3 cm and the inner conductor radius in the coaxial case is r_c = 5.8 cm. In each case, we will present a series of simulations of a constant impedance beam for which the current is varied from 16 kA to 26.7 kA (V_o = 500 to 850 kV). Note that in the simulations, the inner and outer cavities in the coaxial geometry have the same radial and axial dimensions. Because of the variation of cavity volume, etc. with radius, these cavities are not precisely tuned to one another. This is allowable in the simulations because the numerical cavities are quite lossy (Q of order 10) and have a wide bandwidth. Note also that the simulations in the hollow drift tube geometry were discussed in Ref. 5. In that paper, we found that as the current is increased, the rf current level saturates, perhaps due to beam loading effects. These issues were addressed in some detail, but have not been completely resolved. Here, we only note that the saturation persists in the new geometry.

Each simulation proceeded as follows. The first cavity was driven by an external RF source. starting at t = 0 nsec. The low Q of the numerical cavity was such that at t = 6 nsec, the fundamental TEM mode of the cavity saturates, producing a gap voltage of 40 kV at a frequency f = 1.24 GHz (f = 1.42 GHz in the coaxial case). At this time the beam was injected

with a current rise time of 5 nsec. The simulation continues until t = 20 nsec in the hollow drift tube runs and until t = 18 nsec in the coaxial runs. The shorter time in the coaxial cases was dictated by unstable particle "noise" which grew such that it would interfere with the results for t > 18 ns.

In the hollow drift tube cases, the return current path crosses the radial transmission line from which rf energy is pumped into the first cavity. The impedance of this transmission line is 6.25 ohms, so that the dc energy of the beam is lowered as it crosses the first gap. In the coaxial case an alternate return current path is available such that very little of the dc beam energy is lost at the first gap. Injection energies for the 16, 21.3 and 26.7 kA beams were chosen such that the total dc beam energies were approximately 500, 675, and 850 keV after the first gap for both the hollow drift tube and coaxial geometries. This variation in dc voltage on the beam does not effect the small-signal current modulation from the first gap. The gaps are located at z = 2.8 and z = 34.8 cm. In each case the first gap voltage was V_{10} = 45 kV.

Current modulation was analyzed as

$$I(t) \simeq I_0 + I_1 \sin(\omega t) + I_2 \sin(2\omega t) + \ldots\ldots$$

where $\omega = 2\pi f$. Current modulation at the fundamental frequency, I_1, is plotted versus z in Figs. 3 and 4 for the hollow drift tube and coaxial cases respectively. In each case, the first gap produced rf current I_1 in the 1 to 2 kA range. Values were within 10% of the theoretical predictions from small signal theory for the hollow drift tube case and within 20% for the coaxial case.

As in the previous studies, the partially modulated beam energized the second cavity in such a way as to generate very high voltages and very high current modulation, as is clear from Figs. 3 and 4. These voltage and current modulation levels quickly reached a steady-state level which was very stable from cycle to cycle. In fact, the second cavity modulation differed only in the details, such as gap voltage and modulated beam energy, in ways easily suggested by the theory. Table 1 shows the threshold voltage for full current modulation, from Eq. (12), and the second gap voltage as measured in the simulations. Except for the 26.7 kA runs, where the interaction saturated, the second gap voltage builds up to the point that it surpasses the threshold voltage but stops short of the formation of a virtual cathode. In fact, a higher threshold voltage appears to allow a higher gap voltage during steady-state operation. For those runs in which $V_g \gtrsim V_{th}$ was observed (the $I_0 = 16$ and 21.3 kA runs), a small population of particles emerged from the gap region with $\beta = \beta_{Nm}$ as expected from theory.

Figures 5 and 6 show current and beam kinetic energy measured at $z = 70$ cm plotted versus time over two cycles for the hollow drift tube and coaxial cases respectively. Both figures are for $I_0 = 16$ kA beams. We see that in both cases the modulated current is highly peaked, indicating strong harmonic content and allowing for efficient energy extraction for high power rf pulse generation. It is also evident that the beam in the coaxial configuration has a higher degree of energy modulation than is observed in the hollow drift tube case. This is caused by the difference in gap voltage and by the fact that the beam potential energy is greater in the hollow drift tube case. Note that because the transit time across the gap is finite, an electron does not gain the full energy, eV_g, but a

10

fraction of this energy, MeV_g, where M is called the coupling coeficient of the gap; M is unity for low current beams and narrow gaps and decreases as the gap length is increased or as the current approaches the critical value. Our results indicate $M \simeq 0.5$, which is larger than can be accounted for via the width of the fringe fields of the gap (effective gap length $\simeq 4$ cm). Instead we recall that for $V_g > V_{th}$, the beam energy drops to the critical value such that the critical current is approached or exceeded once per cycle.

Note that in the coaxial geometry, no TEM mode was observed. By this we mean that a) measurements of E_r and B_θ did not show contributions from sources other than the modulated intense beam and b) the modulation had no unexpected features that might indicate the presence of a TEM mode. We do not consider this a definitive result, however, because of the shortness of the simulation pulse in comparison with a typical laboratory beam pulse.

For completeness, we mention that many of the favorable properties of MIREB generation that were observed in our previous studies appear to be retained in the coaxial geometry. These include:

(1) The bunching mechanism reaches steady-state after a few RF cycles. Phase-space plots, electrostatic potential plots, and modulated current are identical from RF cycle to RF cycle.

(2) Transients are of no importance and reflections are not necessary for the mechanism.

(3) During each cycle, the energy of the beam is decreased at the gap to a critical value at which point theoretical analysis indicates that the propagation of the slow space charge wave is halted and electrons are slowed to a nonlinear limiting velocity, β_{Nm}.

11

(4) Half a cycle later, the energy of the particles is increased beyond the injection value. These particles have a narrow energy spread.

(5) The particle energy, modulated as $E(t) \simeq E_0 + E_1 \sin(\omega t)$, is stable from cycle to cycle. The energy modulation appears to be out of phase with the current modulation, but the fact that the current is in phase with the power shows that the small population of particles at high energy and low current carry very little power.

(6) The beam was not modulated by the full amplitude of the voltage at the second gap, indicating a finite transit time effect. The coupling coefficient, M, appears to be $\simeq 0.5$.

(7) Significant compression of RF power has occurred, with more than 60% of the power compressed into less than 30% of the RF cycle.

Finally, we considered modulation of a very large diameter, $r_b = 26.1$ cm, $I_0 = 100$ kA, $V_0 = 460$ kV beam. The simulation geometry in this case is shown in Fig. 7. With $r_w = 26.4$ and $r_c = 25.8$, the critical current in this case is $I_c = 575$ kA, well in excess of 100 kA. The cavities, located at z = 2.4 and 26.4 cm are tuned to a frequency of f = 1.36 GHz. As before, the external rf is turned on at t=0, and beam injection starts at t = 6 ns, reaching full current at t = 11 ns. The simulation continues until t = 17 ns. Modulated current, I_1 is shown versus z in Fig. 8. Modulation from the first gap voltage, $V_{10} = 20$ kV, reaches $I_1 = 6.5$ kA at a distance of 24 cm from the first gap in good agreement with theory. The second gap voltage reaches a value of 280 kV, approaching the threshold voltage $V_{th} = 330$ kV. The modulated current rises very sharply after the second gap, reaching $I_1 = 68$ kA at the exit of the simulation region at z = 50.4 cm. At this point, the beam carries

31 GW of rf power. As before, the current is highly peaked, indicating a strong harmonic content.

IV. Discussion

We have shown that the essential physics of intense beam modulation carries over to the new geometry. This is an encouraging result. In the simulations where the two geometries were directly compared, the most significant change introduced by the added center conductor was an increase in voltage at the second gap. This increase is suggested by the increase in the threshold voltage for nonlinear disruption of slow space charge wave propagation (Eq. 12). It is interesting to note that there is nothing in the theoretical work to date that specifies that the gap voltage will always build up to a point where the nonlinear threshold voltage is exceeded but not to a point where a virtual cathode is formed. This appears to be the case in the simulations, however. Thus the threshold voltage calculation, crude as it is, indicates scaling for the steady-state gap voltage with beam energy, current, and geometrical factors.

The simulations also revealed differences in the linear regime (first gap) modulation, which were in agreement with the theory. These should not be considered significant, however, because the nature of the second gap interaction is such that the steady state second gap voltage and modulation levels are not affected by small changes in the first gap modulation.

A possible negative impact of the increased gap voltage observed in the coaxial drift tube geometry is the difficulty of avoiding breakdown at the gaps. This has been previously avoided by the convenient property of electrostatic insulation, wherein the space charge potential of the intense beam near the gap provides insulation.[3,13] This has been observed in

simulations and is required to explain the experimental results to date. The practical limits of electrostatic insulation have not yet been determined so it is difficult to predict the effect of a 20% increase in the gap voltage that was observed in several of the simulations presented here. It is important to realize that a great deal of freedom exists to design an experiment with the appropriate values for beam kinetic energy, potential energy, current, and nonlinear threshold voltage such that the desired second gap voltage is obtained.

An additional encouraging result is that no TEM mode was observed. This suggests that the TEM mode does not couple strongly to the cavities, which is not surprising, and further suggests that the TEM mode, if present, would have to reach large amplitude before it could interfere with the electromagnetic isolation of the two cavities. This speculative argument presupposes that the TEM mode is initially zero in amplitude as in the simulations. If a spurious TEM mode proved problematical, preventive measures, such as tuned cavities, could be introduced to disrupt the mode.

Another issue which might be affected by the change to coaxial geometry is the issue of beam loading. It has been suggested[1,5,14], for instance, that nonlinear beam loading may be responsible for the saturation in the modulated current levels. One difficulty here is that significant nonlinear beam loading has been demonstrated as the critical value of the current is approached.[14] At these mildly relativistic energies, however, the ratio I_0/I_c becomes smaller as I_0 increases at constant impedance. With the present results one can speculate that a) because the switch from hollow to coaxial geometry involves a drop by a factor of two in the value of I_0/I_c, nonlinear beam loading effects, which vary strongly with I/I_c, cannot easily explain the way the saturation time at the second gap

14

increases with I_0 and b) whatever effect beam loading has on the steady-state rf voltage and current levels it appears to persist through the change from the hollow to the coaxial geometries. The close agreement between the hollow drift tube geometry simulations presented here and in ref. 5 and the experimental results, also presented in ref. 5, remains somewhat of a mystery. One difficulty is that the Q factor is so low in the simulations (of order 10) in comparison to the experiments (of order 1000) that it is not clear that we should expect agreement in the first place. Relativistic klystron amplifier research would clearly benefit from an enhanced theoretical understanding of beam loading for intense relativistic beams, especially with respect to the applicability of parallel plate models[14-17] to the more complicated geometries considered here.

A point that was not addressed in the simulations is the fact that rich harmonic content is predicted for these highly modulated beams and is observed in the simulations and in the experiments. It has been shown experimentally that through the use of a third, tuned cavity, the ratio of the second harmonic amplitude to the fundamental, I_2/I_1, could be increased from ~ 0.3 to ~ 0.8.[3] Similar results have been demonstrated for the third harmonic in some cases. The difficulty is that with the hollow geometry, these harmonics may be above the cutoff frequency of the drift tube such that the rf power will radiate in an uncontrolled way, reducing the efficiency. In the coaxial drift tube, this problem is easily avoided. This is a further advantage of the coaxial geometry.

Finally, we should comment on the arbitrariness of our choice of 100 kA for the high power modulation result of Figs. 7 and 8. We find nothing in the simulation results that suggests a limitation on the current in this

geometry. In fact we speculate that the rf power carried by the beam in this geometry will be limited only by the experimental difficulties associated with generation and transport of such ultra-high current beams.

Acknowledgments

References

1. M. Friedman, J. Krall, Y.Y. Lau and V. Serlin, Rev. Sci. Instrum. 61, 171 (1990).

2. M. Friedman and V. Serlin, Phys. Rev. Lett. 55, 2860 (1985).

3. M. Friedman, J. Krall, Y.Y. Lau and V. Serlin, J. Appl. Phys. 64, 3353 (1988).

4. M. Friedman and V. Serlin, Appl. Phys. Lett. 49, 596 (1986); M. Friedman, V. Serlin, A. Drobot and A. Mondelli, IEEE Trans., Plasma Sci., PS-14, 201 (1986).

5. M. Friedman, V. Serlin, D. Colombant, J. Krall and Y.Y. Lau, SPIE Tech. Symposium on High Power Lasers and Optical Computing, Los Angeles, CA, 14-19 Jan 1990.

6. M. Friedman, Y.Y. Lau, J. Krall and V. Serlin, "Ultra High Power Relativistic Klystron Amplifiers", Patent Disclosure, Navy Case No. 72517 (January 30, 1990).

7. K. R. Eppley, W. B. Herrmannsfeldt and R. H. Miller, Proc. of the 1987 IEEE Part. Accel. Conf., 1809 (1987).

8. R. J. Briggs, Phys Fluids 19, 1257 (1976).

9. Y. Y. Lau, J. Appl. Phys. 62, 351 (1987).

10. J. Krall and Y. Y. Lau, Appl. Phys. Lett. 52, 431 (1988).

11. Y.Y. Lau, J. Krall, M. Friedman and V. Serlin, IEEE Trans. Plasma Sci. PS-16, 249 (1988).

12. CONDOR is an extension of the MASK computer code developed by A. Palevsky and A. Drobot, in Proceedings of the 9th Conference on Numerical Simulation of Plasmas, Northwestern University, Evanston, IL, 1980 (unpublished).

13. M. Friedman and V. Serlin, IEEE Trans. Electr. Insul. EI-23, 51 (1988).

14. D. Colombant and Y.Y. Lau, Phys. Rev. Lett. 64, 2320 (1990).

15. C. S. Bull, Proc. Inst. Electr. Eng. Part B 104, 374 (1957).

16. M. V. Chodorow and C. Susskind, Fundamentals of Microwave Electronics (McGraw-Hill, New York, 1964), Chap. 3.

17. M. Friedman and V. Serlin, J. Appl. Phys. 58, 1460 (1985).

Run	geometry	I_0(kA)	V_0(kV)	V_{th}(kV)	V_g(kV)
1	hollow	16.0	500	280	420
2	hollow	21.3	675	400	410
3	hollow	26.7	850	525	400
4	coaxial	16.0	500	360	500
5	coaxial	21.3	675	500	490
6	coaxial	26.7	850	645	400

Table 1. Simulation geometry, dc beam current and voltage, nonlinear threshold voltage from Eq. (12) and voltage observed at the second gap is tabulated for each of six simulations.
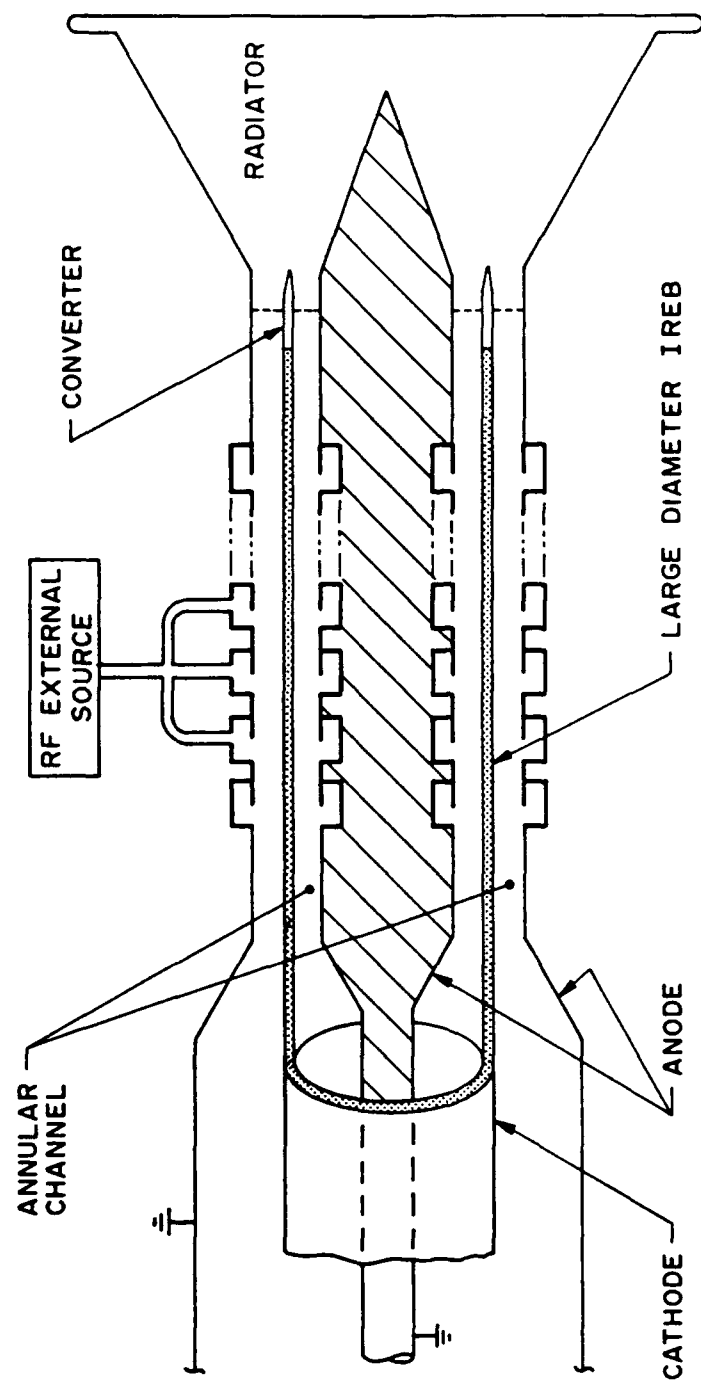
Fig. 1 — Schematic of a multiple-cavity coaxial-geometry relativistic klystron amplifier

19
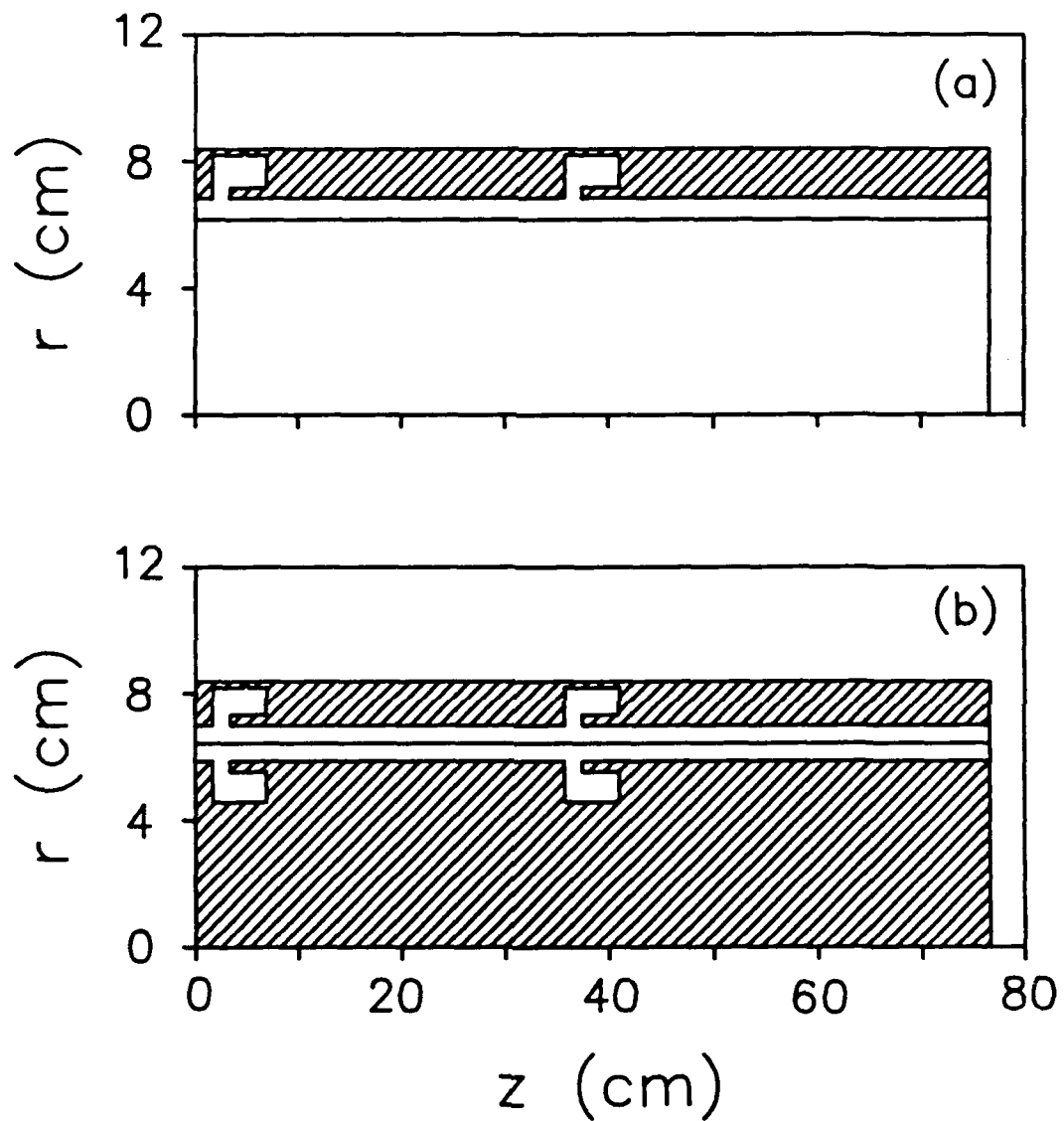
Fig. 2 — Simula.io.. geometry for a) hollow drift tube configuration with outer wall radius 6.8 cm and beam radius 6.3 cm and b) coaxial configuration with outer wall radius 6.8 cm, beam radius 6.3 cm and inner conductor radius 5.8 cm
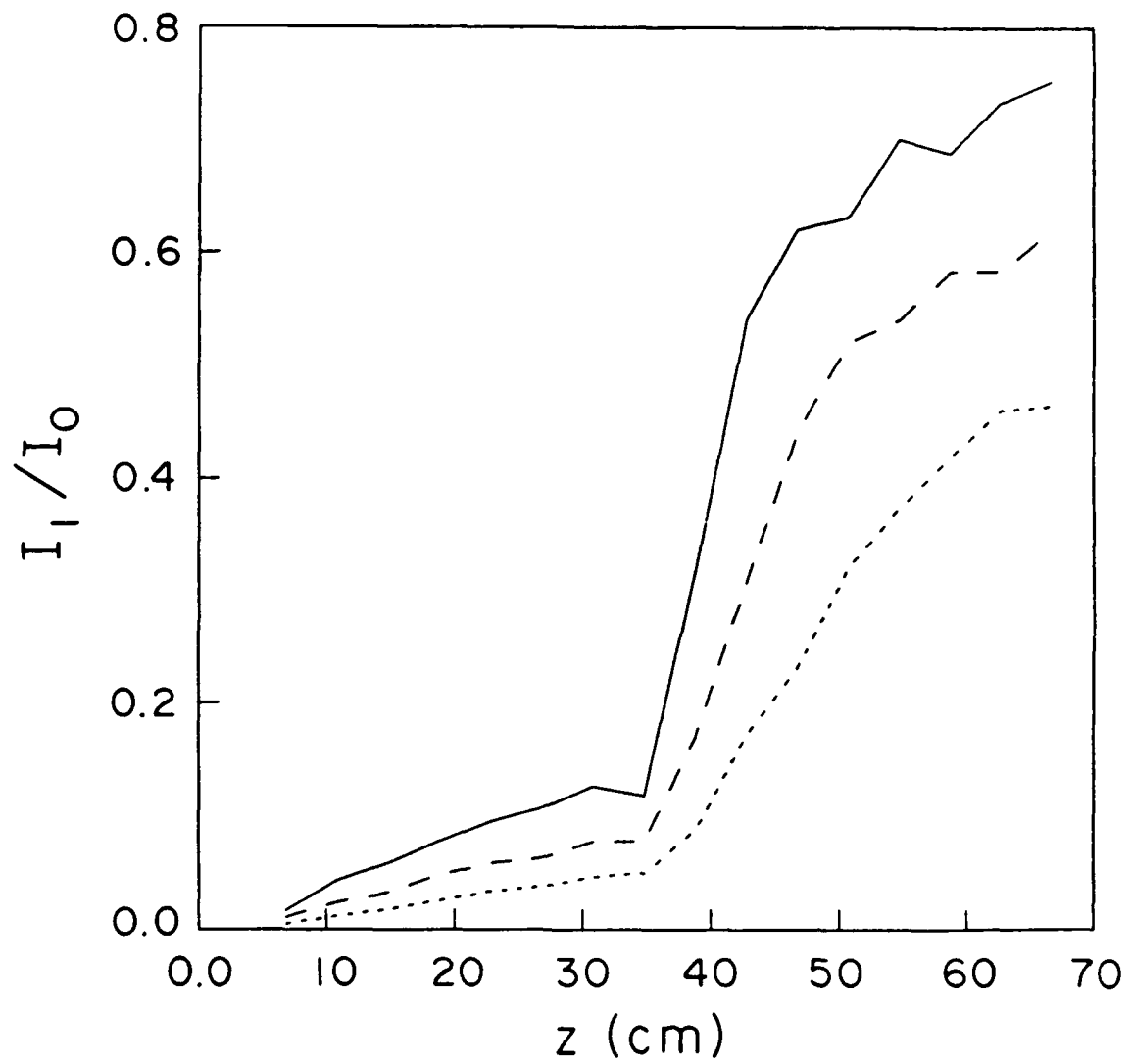
Fig. 3 — Fractional current modulation at the fundamental frequency, I_1/I_0, plotted versus z for the hollow drift tube geometry for $I_0 = 16$ kA, $V_0 = 500$ kV (solid line), $I_0 = 21.3$ kA, $V_0 = 675$ kV (dashed line) and $I_0 = 26.7$ kA, $V_0 = 850$ kV (dotted line).

21
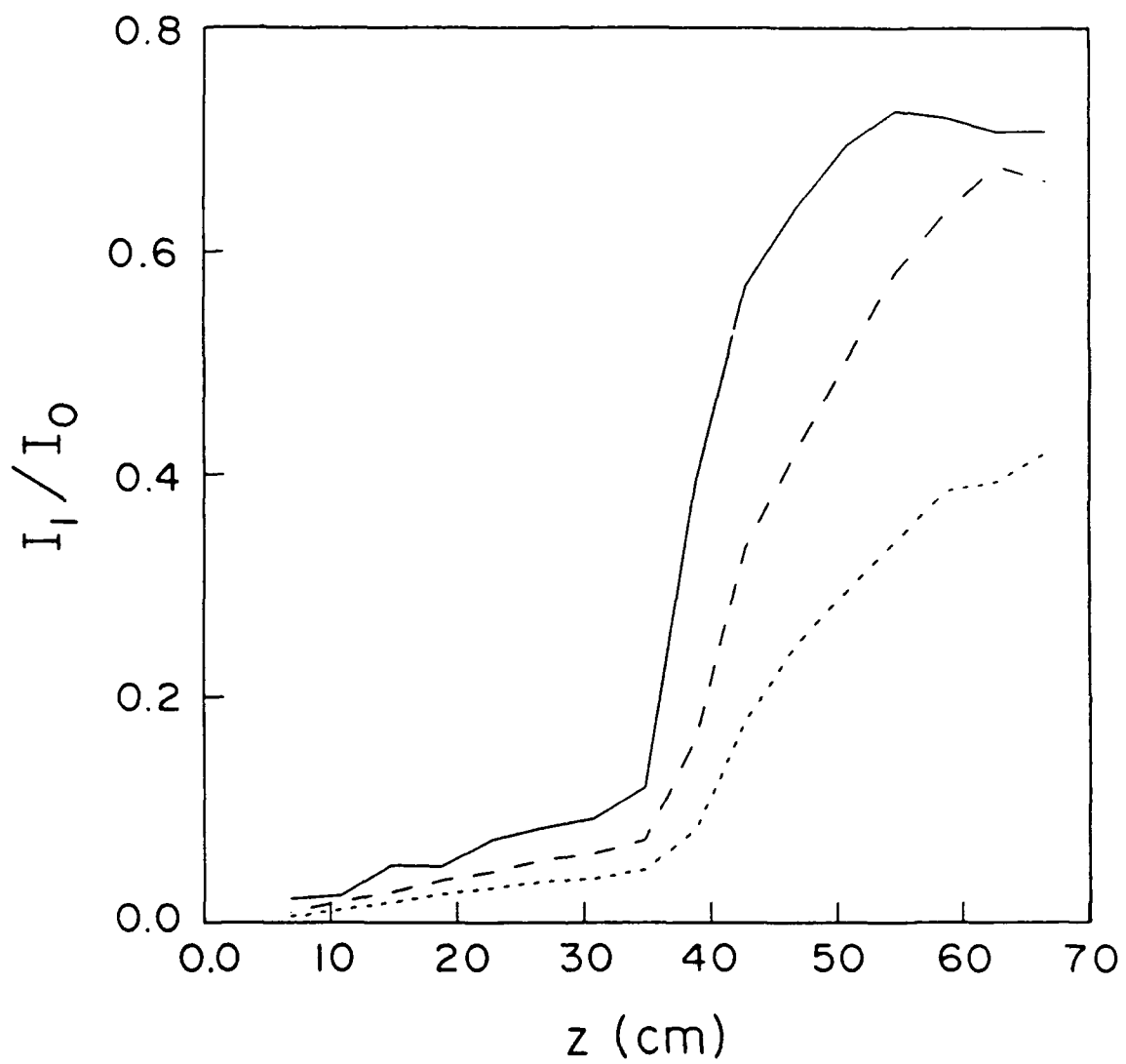
Fig. 4 — Fractional current modulation at the fundamental frequency, I_1/I_0, plotted versus z for the coaxial drift tube geometry for $I_0 = 16$ kA, $V_0 = 500$ kV (solid line), $I_0 = 21.3$ kA, $V_0 = 675$ kV (dashed line) and $I_0 = 26.7$ kA, $V_0 = 850$ kV (dotted line).
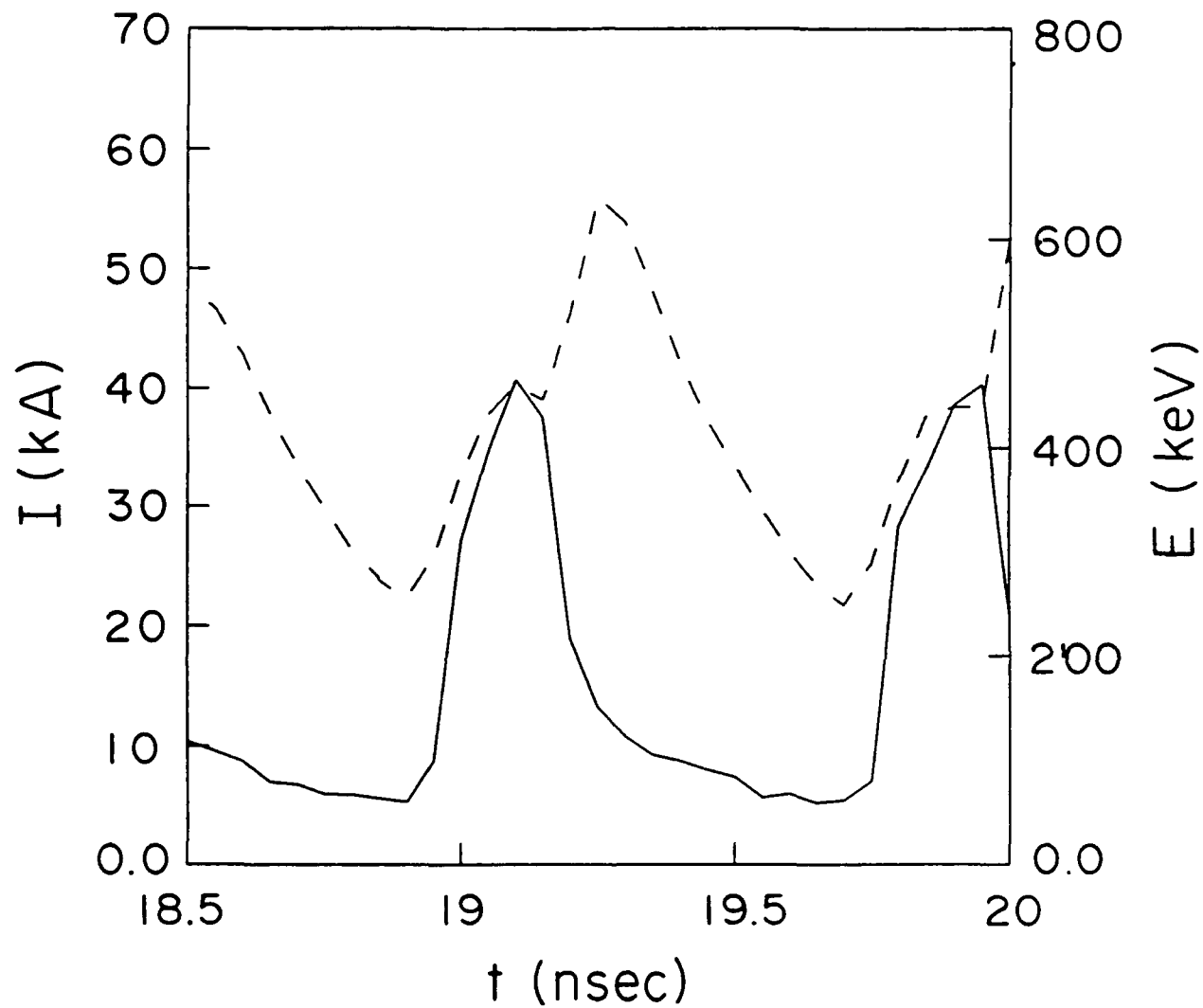
Fig. 5 — Beam current (solid line) and kinetic energy (dashed line) measured at z = 70 cm and plotted versus time over two cycles for the hollow drift tube case. Here, I_0 = 16 kA and V_0 = 500 kV.

23
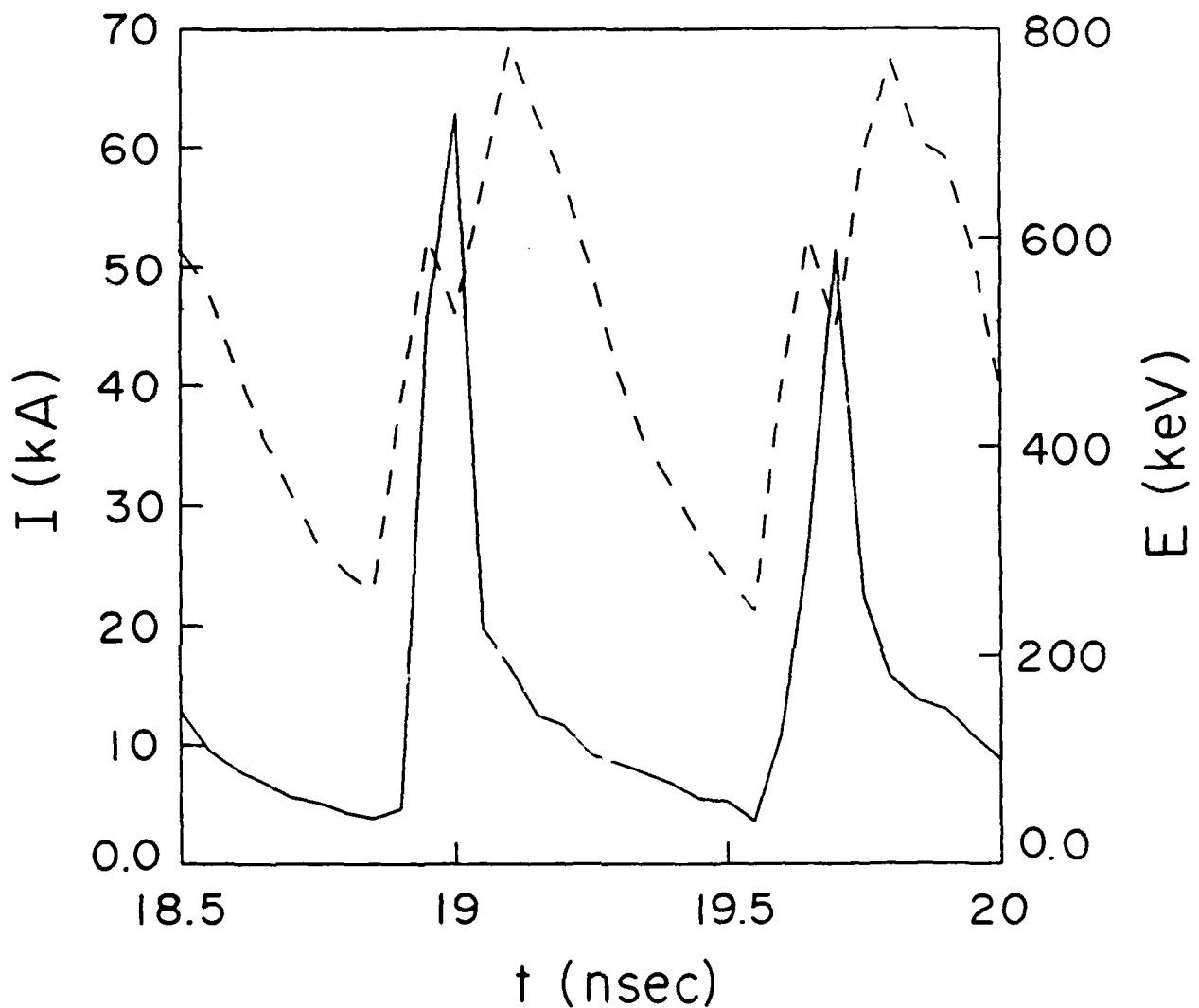
Fig. 6 — Beam current (solid line) and kinetic energy (dashed line) measured at z = 70 cm and plotted versus time over two cycles for the coaxial drift tube case. Here, I_0 = 16 ka and V_0 = 500 kV.
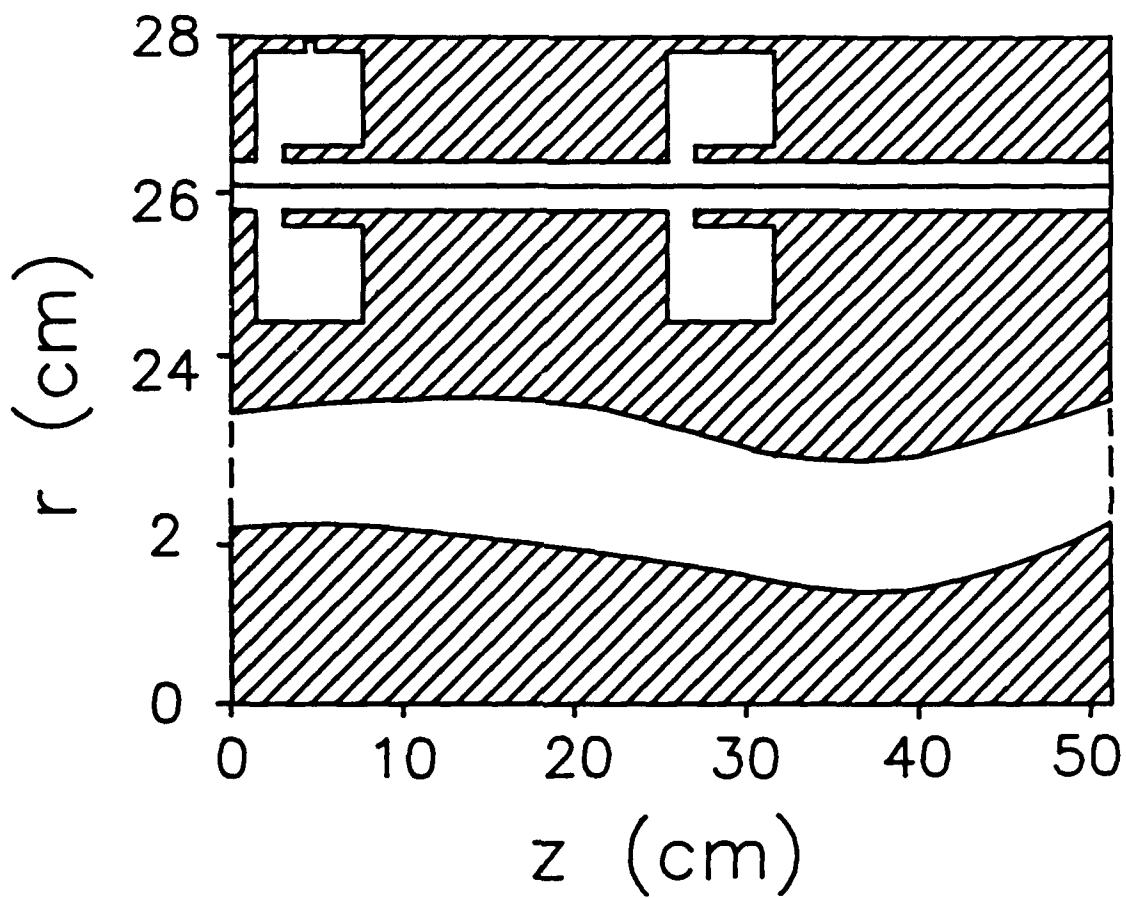
Fig. 7 — Simulation geometry for high current modulation with outer wall radius 26.4 cm, beam radius 26.1 cm and inner conductor radius 25.8 cm
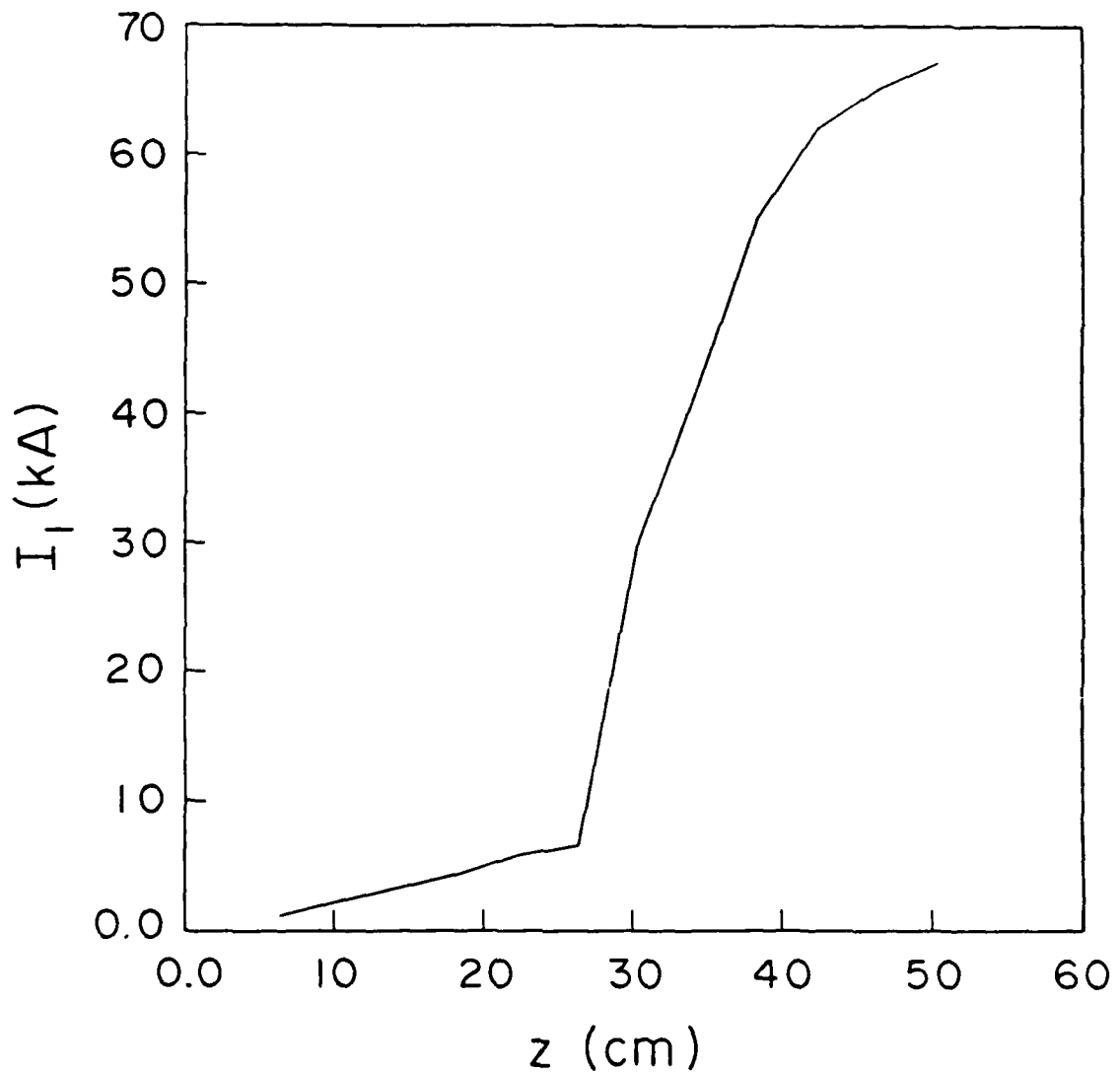
Fig. 8 — Modulated current amplitude, I_1, plotted versus z for an $I_0 = 100$ kA, $V_u = 460$ kV beam